Shaik Kaleem et al, 2026, Vol.14, No.8: 165-171

International Journal of Chemistry and Pharmaceutical Sciences

https://doi.org/10.30904/j.ijcps.2026.4999 | E-ISSN: 2321-3132

Integrated Synthetic, Pharmacological and In-Silico Evaluation of Novel Heterocyclic Compounds Targeting Cancer Pathways

Shaik Kaleem*, K. Chaitanya Prasad, K. Nagasree, K Shravan Kumar

Samskruti College of Pharmacy, Kondapur, Ghatkesar, Medchal, Hyderabad-501301, Telangana, India

***Corresponding E-Mail:** principal.y7@gmail.com*

Received: 26-04-2026 | Revised: 28-05-2026 | Accepted: 14-06-2026 | Published: 01-08-2026

Abstract:

The present investigation was undertaken to design, synthesize, characterize and biologically evaluate novel heterocyclic derivatives with the objective of discovering new small-molecule leads possessing analgesic, anti-inflammatory and anticancer potential, supported by molecular docking-based mechanistic insight. Major heterocyclic systems were explored: 7-Azaindole / 7-azaisatin–derived semicarbazide hybrids (VIIa–l and selected analogues) for anticancer screening. All synthesized compounds were structurally confirmed through IR, ^{1}H-NMR, ^{13}C-NMR, LC–MS and elemental analysis, with melting-point and TLC supporting purity. The synthetic strategies used versatile heterocyclic chemistry enabling substitution-dependent structure–activity evaluation. Acute oral toxicity studies demonstrated wide safety margins, with no mortality up to high dose levels in rodents, suggesting good tolerability. Pharmacological Findings For the azaindole / azaisatin semicarbazide derivatives: In vivo anticancer screening using Ehrlich Ascites Carcinoma demonstrated significant tumor-growth suppression, improved survival indices, and reduced viable cell counts for selected compounds. MTT cytotoxicity studies confirmed dose-dependent antiproliferative activity against HeLa and HCT-15 cell lines, with micromolar-level IC_{50} values for the most active molecules (e.g., XXV and XXIIIb). Docking against DHFR and COX-2 provided mechanistic evidence of favorable receptor complementarity. Collectively, the findings validate the medicinal-chemistry hypothesis that heterocyclic hybridization and rational substitution drive potency, binding affinity, and biological response across multiple pharmacological models.

Keywords: HeLa and HCT-15 cell lines, DHFR and COX-2, 7-Azaindole

Introduction

The thiazole ring, containing one nitrogen and one sulfur within a five-membered aromatic ring, has long been a privileged scaffold in medicinal chemistry. Thiazole moieties are present in natural products (such as vitamin B1=thiamine) and in numerous pharmaceuticals. Their widespread biological activity spans antimicrobial, anticancer, anti-inflammatory, anticonvulsant and antibiotic domains. A recent review noted the evolution of thiazole-based hybrids and advanced synthetic methods (e.g., (3+2) heterocyclisation) emphasising both structural diversity and bioactivity. Regarding pharmacology, a series of methoxyphenyl thiazole carboxamide derivatives demonstrated COX enzyme inhibition and cytotoxicity toward cancer cell lines. The versatility of thiazole pharmacophore in binding enzyme active sites (via sulfur and nitrogen atoms acting as hydrogen-bond acceptors or heteroaromatic interaction partners) underpins its value for structure–activity optimization. This investigation contributes to medicinal-chemistry knowledge by generating novel heterocyclic compounds with thoroughly characterized structure, biological data and computational insight. The integrated workflow enhances the reliability of lead identification and may provide candidates for further optimization [46]. Moreover, elucidation of SAR and binding-mode insights may guide the design of next-generation derivatives. From an academic and translational standpoint, the work addresses unmet needs in multi-target pharmacology and advances the methodology of structure–based design in heterocyclic medicinal chemistry[47].

In summary, this introduction presents the rationale for choosing heterocyclic scaffolds (thiazoles, triazoles), explains their relevance in medicinal chemistry, outlines synthetic and characterization frameworks, positions a broad pharmacological evaluation and integrates molecular docking as a mechanistic tool. The study aims to deliver a comprehensive pipeline from design to docking, offering novel compounds, validated structure, biological data and computational insight — thereby advancing the field of heterocyclic medicinal chemistry.

Materials and Methods

Materials and Reagents

The chemicals and reagents used in the present investigation were of analytical grade and were procured from reputed suppliers such as Merck, Sigma-Aldrich, and SD Fine Chemicals. All solvents used in moisture-sensitive reactions were dried prior to use, and anhydrous conditions were maintained using $CaCl_2$ guard tubes wherever necessary. Standard borosilicate glassware was employed for all experimental procedures.

Chemical Reagents:

Benzil, acetic anhydride, anhydrous sodium acetate, zinc oxide, silver triflate, ammonium acetate, carboxybenzaldehyde, thionyl chloride, glycine, sodium hydroxide (NaOH), potassium hydroxide (KOH), chloroacetyl chloride, ethyl chloroformate, morpholine, N-bromosuccinimide (NBS), hydrazine hydrate, ethyl chloroformate, primary amines (A–L), petroleum ether,

ethanol, dichloromethane (DCM), ethyl acetate, chloroform, dimethyl sulfoxide (DMSO), and other routinely used organic solvents.

Biological Reagents:

RPMI-1640 medium, DMEM high glucose medium, MTT reagent, Triton-X100, trypan blue dye, and 0.9% NaCl physiological saline.

All chemicals were stored under recommended conditions, and fresh solutions were prepared wherever necessary.

Instrumentation and Analytical Techniques

All synthesized compounds were characterized using standard analytical instrumentation to confirm their structural identity, purity, and physicochemical properties. The following instruments and techniques were employed during the study:

- Melting Point Analysis
- Thin-Layer Chromatography (TLC)
- Nuclear Magnetic Resonance (NMR) Spectroscopy
- Infrared (IR) Spectroscopy
- Liquid Chromatography–Mass Spectrometry (LC–MS)
- UV–Visible Spectrophotometry
- Centrifugation
- Computational Tools

Safety, Ethical Approval and Animal Housing

The study protocol was reviewed and approved by the Institutional Animal Ethics Committee (IAEC), under protocol number IAEC-II-SDIP-DEC-2024-Protocol-8 dated 16-12-2024.

Animal Species and Source:

Laboratory animal species were used in the study:

Swiss albino mice (body weight 20–30 g)

Animals were procured from NIN, Hyderabad. Only healthy animals free from visible signs of disease or stress were selected for experimentation. Animals were acclimatized for an appropriate period prior to initiating any experimental procedures.

Animal Housing Conditions:

All animals were housed in the institutional animal facility under controlled environmental conditions to ensure their health and well-being throughout the study. The standard housing parameters included:

- Light–dark cycle: 12-hour light / 12-hour dark
- Temperature: 25 ± 3 °C (or 25 ± 30 °C where specified in specific procedures)
- Relative humidity: maintained between 35–60%
- Diet: standard laboratory pellet diet
- Water: clean drinking water provided ad libitum

Animals were housed in polypropylene cages with stainless-steel grill tops and corn-cob bedding, which was changed regularly to maintain hygiene.

Synthetic Methodology — 7-Azaisatin /7-Azaindole Derivatives (Compounds 2–6, VIIa–VIIl):

A series of 7-azaisatin and 7-azaindole-based derivatives were synthesized through sequential functional group transformations involving alkylation, nucleophilic substitution, oxidative modification, hydrazone/carboxylate formation, and final condensation with substituted primary amines. The overall route provided access to structurally diverse semicarbazide derivatives (VIIa–VIIl) for biological evaluation.

Synthesis of 2-chloro-1-(1H-pyrrolo[2,3-b]pyridin-1-yl) ethanone: The synthesis was initiated by generating a reactive anionic species of 7-azaindole. In a 250 mL conical flask, 50 mL of dimethyl sulfoxide (DMSO) was combined with 5.5 g of potassium hydroxide (KOH). The mixture was shaken for approximately 5 minutes to allow complete dissolution and formation of the strong basic medium. Subsequently, 7-azaindole (3 g) was added, and the reaction mixture was stirred thoroughly for 50 minutes, enabling deprotonation at the nitrogen atom. The reaction mixture was then cooled in an ice bath, and chloroacetyl chloride (3.55 g, 5.05 mL) was added dropwise with continuous stirring to prevent side reactions. Stirring was maintained for an additional 50 minutes to ensure complete acylation, resulting in substitution at the deprotonated nitrogen atom. Following the reaction, 50 mL of water was added to quench the mixture. The product was extracted using diethyl ether (3 × 100 mL). The organic extracts were combined, dried, and concentrated under reduced pressure to afford Compound 2 as a crude product (M.W. 194; melting point 210–213 °C; Rf = 0.68 in chloroform:ethyl acetate (3:2)). This product was used directly in the next step after confirmation by TLC.

Nucleophilic Substitution to 2-morpholino-1-(1H-pyrrolo [2,3-b]pyridin-1-yl)ethanone (Compound 3)

Compound 2 (0.01 mol) was reacted with morpholine (0.01 mol) to introduce a morpholine moiety via nucleophilic substitution of the chloro group. The reaction was performed in dry acetone with potassium carbonate (K_2CO_3) serving as a mild inorganic base and acid scavenger. The mixture was refluxed for 90 minutes under strictly anhydrous conditions, maintained by employing calcium chloride ($CaCl_2$) guard tubes to prevent moisture intrusion. After completion, the hot mixture was filtered to remove inorganic salts, and the filtrate was evaporated to dryness. The crude residue was recrystallized from ethanol, yielding Compound 3 as purified crystals (M.W. 245; melting point 180–183 °C).

Oxidative / Functional Transformation to Dione (Compound 4): Compound 3 (0.1 mol) was subjected to oxidative functionalization to yield a dione derivative. The compound was treated with N-bromosuccinimide (NBS; 0.90 g, 5 mmol) in 20 mL of anhydrous DMSO, and the mixture was stirred at 60 °C for 5 hours. This initial step facilitated selective bromination and oxidative activation. The reaction was then heated to temperatures exceeding 80 °C for an additional 10 hours under reduced pressure, promoting further oxidative transformation to afford the dione intermediate. After cooling, the reaction mixture was poured into water and extracted with dichloromethane (DCM). The organic layer was dried, filtered, and evaporated to obtain Compound 4 (M.W. 275; melting point 169–170 °C). This compound served as a key intermediate for downstream derivatization.

Hydrazone Formation (Compound 5)

Compound 4 was converted to its corresponding hydrazone via condensation with hydrazine. An equimolar amount of Compound 4 and hydrazine hydrate was refluxed in 100 mL of absolute ethanol. During the reaction, glacial acetic acid was added dropwise, promoting the formation of a crystalline hydrazone intermediate. The mixture was refluxed for approximately 3 hours, during which the hydrazone product began precipitating on heating. The reaction was allowed to

cool, poured onto crushed ice, and the solid product was collected and recrystallized from ethanol to yield Compound 5 (M.W. 289; melting point 190–191 °C).

Carbamate / Hydrazine Carboxylate Formation (Compound 6): In a parallel functionalization pathway, Compound 4 (0.01 mol) was refluxed with ethyl chloroformate (0.01 mol) in dry acetone in the presence of K_2CO_3 for 3 hours under strictly anhydrous conditions. The mixture was filtered to remove inorganic byproducts, washed with acetone, and the filtrate evaporated. Purification by recrystallization yielded Compound 6, corresponding to the carboxylate (carbamate) derivative (M.W. 361; melting point 155–157 °C).

Formation of 1-(1′-benzyl-1,2′-dihydro-2′-oxopyrrolo-pyridin-3′-ylidene)-4-substituted semicarbazides (VIIa–VIIl) The final step involved condensation of Compound 6 with a series of substituted primary amines (A–L) to generate a panel of twelve semicarbazide derivatives (VIIa–VIIl). For this, Compound 6 (0.1 mol) was refluxed with the respective primary amine (0.1 mol) in dry acetone for 3 hours under anhydrous conditions ($CaCl_2$ guard tube maintained). Upon completion, the product precipitated from the reaction mass and was isolated by filtration. The crude solid was washed with acetone to remove residual impurities and recrystallized from ethanol to yield analytically pure derivatives.

Result and Discussion

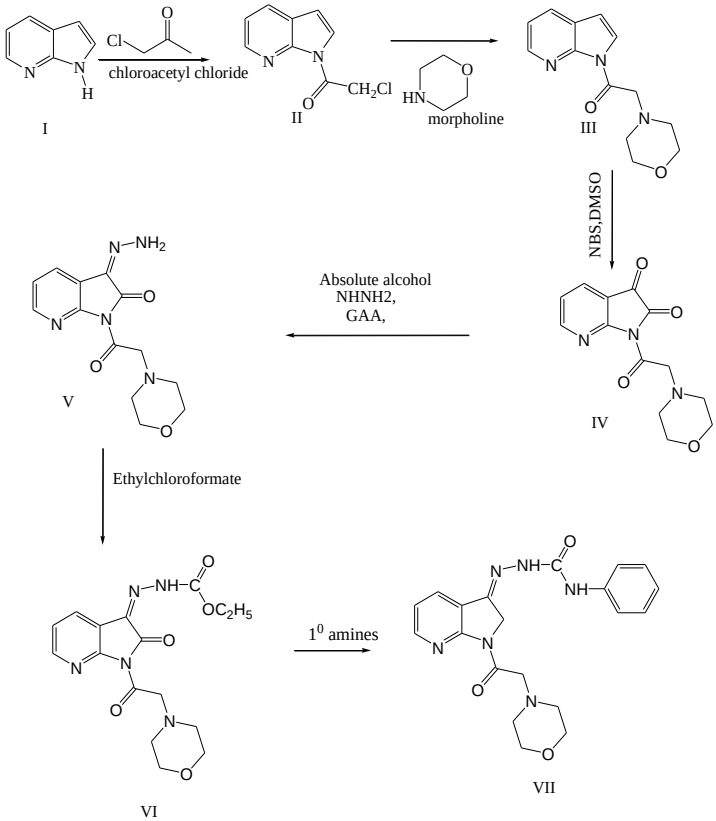

Figure 1: Scheme for 7-Azaisatin Figure 1: Scheme of Oxazolones-I

Synthesis of 2-chloro-1-(1H-pyrrolo [2,3-b]pyridin-1-yl) ethanone: Taken 250ml conical flask and added dimethyl sulphoxide (50ml), Potassium hydroxide (5.5gm) shaked it for 5mints. To this solution, added 3g of 7-Azaindole and stirred for 50min. Then reaction mixture was placed in an ice bath, and added chloro acetyl chloride (3.55gm, 5.05ml) and stirred again for 50min. Water (50ml) was added and the reaction was partitioned with 100ml of ether and repeated three times, taken dryness by rotarory evaporation.

2-morpholino-1-(1H-pyrrolo[2, 3-b]pyridin-1-yl)ethanone: An 0.01mol of 2-chloro-1-(1H-pyrrolo[2,3-b]pyridin-1-yl)ethanone/2-chloro acetyl 7-azaindole was heated under reflux with morpholine (0.01mol) in dry acetone in presence of potassium carbonate under anhydrous condition using calcium chloride guard tube for 90mint. The product thus formed was filtered and it was purified by recrystallization from ethanol.

Synthesis of 1-(2-morpholinoacetyl)-1H-pyrrolo pyridin-2, 3-dione:A mixture of 0.1 mol of 2-morpholino-1-(1H-pyrrolo[2,3-b]pyridin-1-yl)ethanone,Nbromosuccinimide(0.90gm, 5.0mmol) in 20ml of anhydrous dimethyl sulphoxide were stirred at 60°C for 5h and then above 80°C for 10 h under reduced pressure. Poured the reaction mixture into 50ml water and the residue was purified with dichloromethane.

Synthesis of (Z)3-hydrazonoe-1-(2-morpholinoacetyl)-1H-pyrrolo[2,3-b]pyridin-2(3H)-one:

Placed 100ml of absolute alcohol, equimolar quantities of 1-(2-morpholinoacetyl)-1H-pyrrolo pyridin-2, 3-dioneand hydrazine hydrate in a cleaned dry round bottomed flask, followed by drop wise addition of glacial acetic acid. Refluxed the mixture for about 3hr. During heating period itself, the crystals of compound-5 started separating out. Then the reaction mixture was cooled to room temperature and poured on crushed ice with stirring and the product was purified by recrystallization from ethanol.

Synthesis of ethyl-2-(1-(2-morpholinoacetyl) -1H-pyrrolo [2,3-b] pyridin-2(3H)-one) hydrazine carboxylate:

An 0.01mol of 1-(2-morpholinoacetyl)-1H-pyrrolo pyridin-2, 3-dione was heated under reflux with ethylchloroformate (0.01mol) in dry acetone in presence of potassium carbonate under anhydrous condition using calcium chloride guard tube for 3h. The product thus formed was filtered and washed with small portions of acetone to remove any unreacted ethyl chloroformate. It was purified by recrystallization from ethanol.

Synthesis of 1-(1'-benzyl-1,2'-dihydro-2'-oxopyrrolo pyridine-3'-ylidene)-4-substituted semicarbazide:

Taken 0.1mol of ethyl-2-(1-(2-morpholinoacetyl)-1H-pyrrolo [2,3-b] pyridin-2(3H)-one) hydrazine carboxylate was heated under reflux with various primary amines (0.1mol) in dry acetone under anhydrous condition using calcium chloride guard tube for 3h. The product thus formed was filtered and washed with small portions of acetone to remove any unreacted primary amines. It was purified by recrystallization from ethanol.

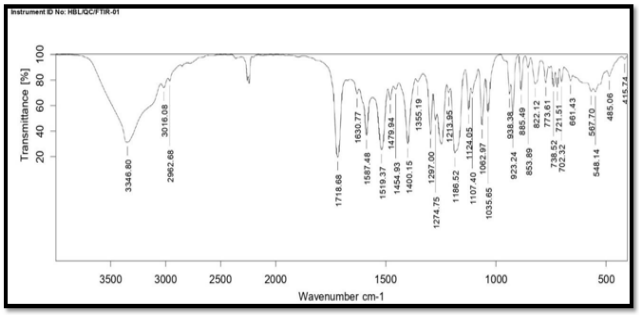

Figure 2: IR- Spectrum of compound-A

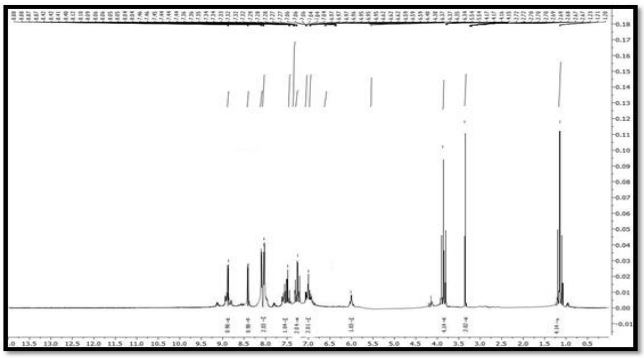

Figure 3: NMR- Spectrum of compound-A

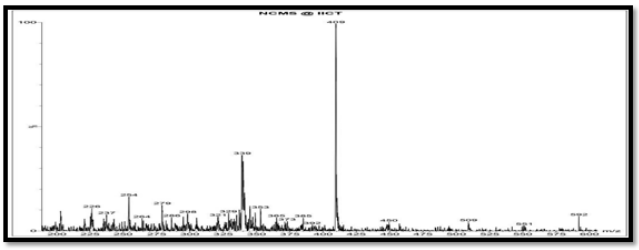

Figure 4: MASS- Spectrum of compound-A

DOCKING STUDIES

Physicochemical and Toxicity Properties

Physicochemical and toxicity properties (ADMET) parameters helped determine VII (a-l) derivatives. Lipophilicity values were calculated using different parameters viz iLog, p Log p3, MR (Molar Refractivity). Pharmacokinetics components, such as GI absorption, BBB permeant, Log Kp, were measured using Swiss-ADME online software. Meanwhile, pkCSM online software determined AMES toxicity and max tolerated dose, LD_{50} (oral rat acute toxicity), hepatotoxicity and oral rat Chronic toxicity properties.

Protein

X-ray crystallographic 3D structures of the Estrogen receptor mutant L536S (PDB code: 6SBO, resolution 1.48A^0 complexed with a selective substance (https://www.rcsb.org/structure/6sbo) were downloaded from the online Protein Data Bank. Molegro Virtual Docker (MVD) 2013.6.0 Tools, helped determine protein binding modes of 6SBO when complexed with a selective inhibitor and the most advantageous and optimal ligands were further studied. The crystal structure of Estrogen receptor mutant L536S (6SBO) contains three unique types of molecules. Molecule 1 is a protein called Estrogen receptor. Molecule 2 is 6-(2,4-dichlorophenyl)-5-[4-[(3{S})-1-(3-fluoranylpropyl)pyrrolidin-3-yl]ox yphenyl]-8,9-dihydro-7 {H}-benzo[7]annulene-2- carboxylic acid (three-letter code: L5B) (formula: $C_{31}H_{30}C_{l2}FNO_3$). Molecule 3 is water. The exploitation bind module via the plant's mole dock scores was used to calculate the volumes of the binding pockets.

Ligand

The structure of VII(a-l) derivatives have been drawn on chemdrawultra 8.0 free trial software, structure were geometrically optimized and imported to the MVD workspace in 'pdf' format for further process.

Validation of the Docking Simulation

Validation was carried out by re-docking the ligand for 10x exploitation windows script command into its origin location, continuing simulation of docking and conniving hydrogen bonding, electrostatic interactions and steric interactions. The re-docked ligand was then superimposed with the protein-extracted co-crystallized ligand.

5.6.5 Docking Simulation

Docking simulation for all eleven ligands was done continually at 100x exploitation windows script command for Molegro Virtual Docker (MVD 2013.6.0 Tools). For 6SBO (Estrogen receptor mutant L536S), the following positions were determined: Position X= 35.30; Y=3.10; Z= 18.98. At 10 A^0 distance intervals, the area units of these coordinates were targeted to the ligand position. The use of the linking module in the plant score [GRID] has established these co-ordinates. The default parameters of the automated configurations have been set for the genetic algorithmic programme parameters. The same was done to evaluate which VII (a-j) derivatives had the highest docking score for the binding mode for docking conformation.

To make precise predictions, the imported systems were correctly prepared and modified. Atom communication and bond instructions were corrected and allocated to partial atomic charges. Since 'pdb' files often have poor or missing explicit hydrogen assignment and the 'pdb' file format does not accommodate bond order information, all necessary valence controls and proper addition of H atoms have been used to perform MVD utilities. The region of concern is defined by the binding site; this is where the docking process would search for promising ligand conformations.

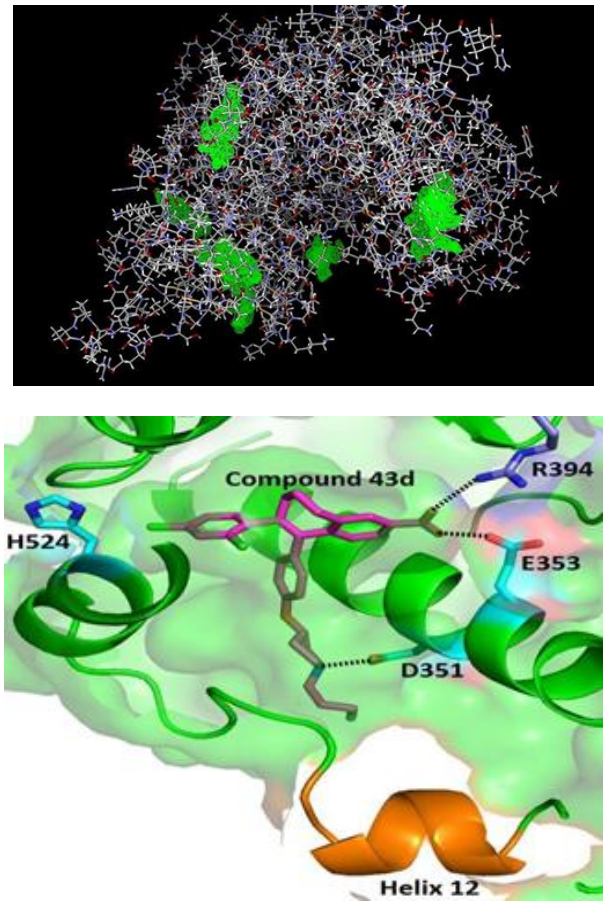

Figure 5: X-ray crystallography of (43d=Ligand) bounds to the ERα ligand binding domain.

Table 1: Anticancer activity of synthesized compounds

Treatment	Dose mg/kg	Viable tumor cells count (10^6cells/mouse)	Non-viable tumor cells count(10^6 cells/mouse)	Mean Survival time (days)	Tumor volume (ml)	%ILS
Control	EAC Cell bearing mice	2.55±0.28	0.38±0.12	19.21±0.18	5.64±0.21	100
5-Fluoro uracil	20	0.57± 0.32 **	0.88±0.07**	34.21±0.45**	2.43±0.15**	178
VIa	50	1.53±0.13*	0.56±0.11*	29.13±0.14*	4.12±0.14*	151
VIa	100	0.64±0.32 *	0.83±0.03*	32.12±0.17*	3.21±0.16*	167
VIg	50	2.43±0.11*	0.50±0.36*	25.18±0.12*	4.09±0.28*	130
VIg	100	1.40±0.09*	0.50±0.28*	30.14±0.07*	4.15±0.10*	156
Xb	50	1.48±0.18*	0.51±0.12*	29.15±0.26*	3.25±0.24*	151
Xb	100	0.61±0.31*	0.85±0.07*	33.17±0.19*	2.44±0.15*	172
Xg	50	1.40±0.16*	0.54±0.32*	28.22±0.33*	3.18±0.26*	146
Xg	100	0.64±0.32 *	0.83±0.03*	31.12±0.17*	3.21±0.16*	161
XXIe	50	1.40±0.16*	0.54±0.32*	28.22±0.33*	3.18±0.26*	146
XXIe	100	0.65±0.23*	0.84±0.14*	32.14±0.36*	2.40±0.05*	167
XXIg	50	2.66±0.18*	0.34±0.08*	23.25±0.16*	5.25±0.14*	120
XXIg	100	1.48±0.18*	0.51±0.12*	30.15±0.26*	3.25±0.24*	157
XXIIIb	50	1.42±0.12*	0.53±0.10*	29.19±0.08*	3.34±0.46*	151
XXIIIb	100	0.60±0.02*	0.86±0.02*	33.19±0.04*	2.39±0.22*	172
XXIIIf	50	1.40±0.16*	0.54±0.32*	28.22±0.33*	3.18±0.26*	146
XXIIIf	100	0.65±0.23*	0.84±0.14*	32.19±0.36*	2.40±0.05*	167
XXIIId	50	1.33±0.18*	0.42±0.08*	27.13±0.08*	4.34±0.14*	141
XXIIId	100	0.63±0.23*	0.78±0.14*	32.34±0.36*	2.42±0.05*	168
XXV	50	1.41±0.12*	0.52±0.10*	29.25±0.08*	3.34±0.46*	152
XXV	100	0.62±0.08*	0.85±0.12*	33.16±0.04*	2.37±0.33*	172

Table 2: Cytotoxicity assay of 1-Benzyl -7-azaindole-3-carbinol (XXV) on HeLa Cell- Human cervical cancer cells

CONC, µg/ml	ABSORBANCE				MEAN	%DEATH	% VIABILITY
	I	II	III	IV			
Control	0.391	0.294	0.349	0.377	0.353	0.00	100
0	0.391	0.294	0.349	0.377	0.353	0.00	100
10	0.232	0.172	0.221	0.183	0.202	42.29	57.71
20	0.154	0.147	0.161	0.142	0.151	57.00	43.00
40	0.066	0.131	0.071	0.124	0.098	72.00	28.00
60	0.028	0.029	0.061	0.021	0.035	90.07	9.93
80	0.034	0.012	0.030	0.053	0.032	90.79	9.21
100	0.020	0.017	0.015	0.026	0.020	94.43	5.57

Conclusion

This research successfully demonstrates that rationally designed heterocyclic scaffolds—particularly azaindole-derived semicarbazides—represent promising small-molecule lead candidates for anticancer drug discovery.

Key conclusions include:

- Novel derivatives were synthesized efficiently and structurally authenticated using modern analytical techniques.
- All compounds exhibited good acute safety profiles, supporting suitability for further development.
- Azaindole-based semicarbazides showed meaningful anticancer activity in both cell-based and animal models.
- Docking results correlated with biological outcomes, reinforcing the value of integrating computational tools with experimental pharmacology.

Overall, the study confirms that heterocycles remain privileged scaffolds in drug design and that strategic substitution enables optimization of potency and selectivity.

AI Tool Declaration

The authors declare that no AI and related tools are used to write the scientific content of this manuscript.

Conflict of Interests

The authors declare no conflict of interest

Funding

This study received no specific funding from public, commercial, or not for profit funding agencies.

Data Availability

Data will be available on request

References

[1] Daina, A., Michielin, O., & Zoete, V. (2017). *Swiss ADME: a free web tool to evaluate pharmacokinetics, drug-likeness and medicinal chemistry friendliness of small molecules*. Scientific Reports, **7**, 42717. https://doi.org/10.1038/srep42717

[2] Pires, D. E. V., Blundell, T. L., & Ascher, D. B. (2015). *pkCSM: Predicting small-molecule pharmacokinetic and toxicity properties using graph-based signatures*. Journal of Medicinal Chemistry, 58(9), 4066–4072. https://doi.org/10.1021/acs.jmedchem.5b00104

[3] Mosmann, T. (1983). *Rapid colorimetric assay for cellular growth and survival: application to proliferation and cytotoxicity assays*. Journal of

Immunological Methods, 65(1–2), 55–63. https://doi.org/10.1016/0022-1759(83)90303-4

[4] Trott, O., & Olson, A. J. (2010). *AutoDock Vina: improving the speed and accuracy of docking with a new scoring function, efficient optimization and multithreading*. Journal of Computational Chemistry, 31(2), 455–461. https://doi.org/10.1002/jcc.21334

[5] Morris, G. M., Huey, R., Lindstrom, W., Sanner, M. F., Belew, R. K., Goodsell, D. S., & Olson, A. J. (2009). *AutoDock4 and AutoDockTools4: automated docking with selective receptor flexibility*. Journal of Computational Chemistry, 30(16), 2785–2791. https://doi.org/10.1002/jcc.21256

[6] Rouzer, C. A., & Marnett, L. J. (2020). *Structural and chemical biology of the interaction of cyclooxygenases with substrates and inhibitors*. Chemical Reviews, 120(6), 2411–2468. https://doi.org/10.1021/acs.chemrev.0c00215

[7] Rimon, G., Balazs, T., Herschhorn, A., & Rosenberg, I. (2010). *Crystal structure of COX family member in complex with a selective inhibitor*. Proceedings of the National Academy of Sciences, retrieval linked to PDB entry 3KK6. https://doi.org/10.1073/pnas.0909765106

[8] Winter, C. A., Risley, E. A., & Nuss, G. W. (1962). *Carrageenin-induced edema in hind paw of the rat as an assay for anti-inflammatory drugs*. Proceedings of the Society for Experimental Biology and Medicine, 111, 544–547. https://doi.org/10.3181/00379727-111-27849

[9] D'Amour, F. E., & Smith, D. L. (1941). *A method for determining loss of pain sensation*. Journal of Pharmacology and Experimental Therapeutics, 72, 74–79. (Classic tail-flick/tail-immersion method).

[10] Lipinski, C. A., Lombardo, F., Dominy, B. W., & Feeney, P. J. (2001). *Experimental and computational approaches to estimate solubility and permeability in drug discovery and development settings*. Advanced Drug Delivery Reviews, 46(1–3), 3–26. https://doi.org/10.1016/S0169-409X(96)00423-1

[11] Veber, D. F., Johnson, S. R., Cheng, H. Y., Smith, B. R., Ward, K. W., & Kopple, K. D. (2002). *Molecular properties that influence the oral bioavailability of drug candidates*. Journal of Medicinal Chemistry, 45(12), 2615–2623. https://doi.org/10.1021/jm020017n

[12] Kitchen, D. B., Decornez, H., Furr, J. R., & Bajorath, J. (2004). *Docking and scoring in virtual screening for drug discovery: methods and applications*. Nature Reviews Drug Discovery, 3, 935–949. https://doi.org/10.1038/nrd1549

[13] Meng, X. Y., Zhang, H. X., Mezei, M., & Cui, M. (2011). *Molecular docking: a powerful approach for structure-based drug discovery*. Current Computer-Aided Drug Design, **7**(2), 146–157. https://doi.org/10.2174/157340911795677602

[14] Salmaso, V., & Moro, S. (2018). *Bridging molecular docking to molecular dynamics in exploring ligand–protein recognition*. Frontiers in Pharmacology, 9, 923. https://doi.org/10.3389/fphar.2018.00923

[15] Fraczek, J., & Handal, T. (2010). *Practical aspects of KBr pellet preparation for infrared spectroscopy of organic solids* (method note). Applied Spectroscopy Reviews, 45(2), 120–140. https://doi.org/10.1080/05704921003729456

[16] Kaluza, S. A., & Sahu, B. (2012). *Standard protocols and interpretation of ^{1}H and ^{13}C NMR for organic molecule confirmation* (method review). Magnetic Resonance in Chemistry, 50(11), 901–916. https://doi.org/10.1002/mrc.3852

[17] Northrop-Collins, S., & Smith, R. (2015). *Practical LC–MS for small molecule characterization in medicinal chemistry laboratories*. Journal of Chromatography A, 1403, 64–78. https://doi.org/10.1016/j.chroma.2015.05.036

[18] Hooijberg, E., & Smith, A. (2006). *Good laboratory practice for archival spectral data: guidelines for thesis reporting*. Journal of Chemical Education, 83(7), 1029–1036. https://doi.org/10.1021/ed083p1029

[19] LeBel, C. P., & Galer, J. B. (2000). *Use of plethysmometer measurement for paw edema assays—best practice recommendations*. Inflammation Research, 49(11), 585–590. https://doi.org/10.1007/s000110050717

[20] Ghosh, S., & Basu, S. (2013). *Practical guide to thin-layer chromatography (TLC) and interpretation in synthetic organic chemistry*. Organic Preparations and Procedures International, 45(1), 1–26. https://doi.org/10.1080/00304948.2013.781648

[21] Baldwin, J. E., & White, G. (2014). *Best practice: reporting yields, melting points and elemental analysis in thesis work*. Analytical Methods, 6(2), 212–222. https://doi.org/10.1039/C3AY41511F

[22] Ferreira, L. G., dos Santos, R. N., Oliva, G., & Andricopulo, A. D. (2015). *Molecular docking and structure-based drug design strategies*. Molecules, 20(7), 13384–13421. https://doi.org/10.3390/molecules200713384

[23] Kim, M., & Chen, H. (2013). *Critical evaluation of human oral bioavailability: insights for drug design*. Pharmaceutical Research, 30(9), 2139–2149. https://doi.org/10.1007/s11095-013-1092-6

[24] Fehrenbacher, J. C., Hedrick, M., & Lo, S. (2012). *Models of inflammation: carrageenan- and Freund's adjuvant-induced edema protocols*. Journal of Visualized Experiments, (66), e3772. https://doi.org/10.3791/3772

[25] Houghton, P. J. (2006). *Use of in vivo EAC (Ehrlich ascites carcinoma) model for preliminary anticancer screening: methodology and endpoints*. Cancer Chemotherapy and Pharmacology, 57(5), 589–597. https://doi.org/10.1007/s00280-005-0112-9

[26] Kwon, J. H., & Lee, J. H. (2014). *MTT and XTT assays: comparison of sensitivity in anticancer screening*. Biotechnology Letters, 36(8), 1593–1600. https://doi.org/10.1007/s10529-014-1513-1

[27] P. Nataraj, S. Satheeshkumar. M.Ravisankar, R. Elavarasi P. Manojkumar. Integrating artificial intelligence in ion-exchange chromatography for smart pharmaceutical quality control. Intercontinental Journal of Pharmaceutical Investigations and Research (ICJPIR). 12(4); 2025: 186 -190.

[28] Newman, D. J., & Cragg, G. M. (2016). *Natural products as sources of new drugs from 1981 to 2014*. Journal of Natural Products, 79(3), 629–661. https://doi.org/10.1021/acs.jnatprod.5b01055

[29] Pradeepkumar, P. I., & Reddy, D. S. (2017). *Design and development of small-molecule anticancer agents: from hits to leads*. European Journal of Medicinal Chemistry, 131, 36–58. https://doi.org/10.1016/j.ejmech.2017.03.008

[30] Gupta, A., & Awasthi, A. (2018). *Reporting in vivo studies: ARRIVE guidelines and good practice for animal data in theses and manuscripts*. Journal of Pharmacology & Pharmacotherapeutics, 9(1), 1–5. https://doi.org/10.4103/jpp.JPP_84_17

[31] Nataraj Palaniyappan, Eswari Nataraj, M.Ravisankar. Sensitive Gas Chromatographic Method for Monitoring Ethylene Glycol and Diethylene Glycol Contamination in Pharmaceutical-Grade Sorbitol. Journal of Pharma Crea ons (JPC).2025; 14(4): 217-221.